AD-A096 653 WISCONSIN UNIV-MADISON MATHEMATICS RESEARCH CENTER F/G 12/1
NUMERICAL HOPF BIFURCATION TECHNIQUES AND THE DYNAMICS OF THE T--ETC(U)
NOV 80 R F HEINEMANN, A B POORE DAAG29-80-C-0041
UNCLASSIFIED MRC-TSR-2136 NL

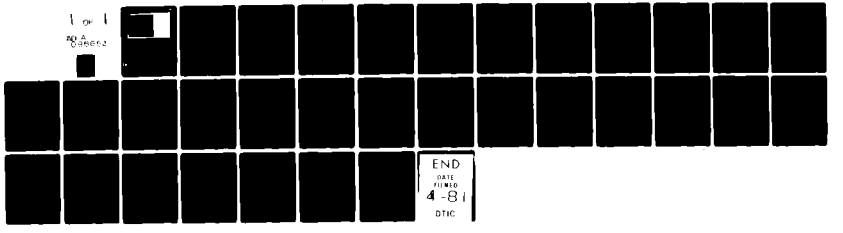

LEVEL II (2)

MRC Technical Summary Report #2136

NUMERICAL HOPF BIFURCATION TECHNIQUES AND THE DYNAMICS OF THE TUBULAR REACTOR MODEL

Robert F. Heinemann and Aubrey B. Poore

Mathematics Research Center
University of Wisconsin—Madison
610 Walnut Street
Madison, Wisconsin 53706

November 1980

Received July 2, 1980

Approved for public release
Distribution unlimited

Sponsored by

U. S. Army Research Office
P. O. Box 12211
Research Triangle Park
North Carolina 27709

UNIVERSITY OF WISCONSIN - MADISON
MATHEMATICS RESEARCH CENTER

NUMERICAL HOPF BIFURCATION TECHNIQUES AND THE DYNAMICS OF THE TUBULAR REACTOR MODEL

Robert F. Heinemann and Aubrey B. Poore

Technical Summary Report #2136
November 1980

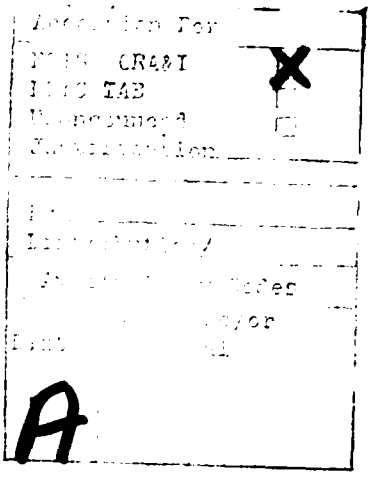

ABSTRACT

Numerical bifurcation techniques were developed for studying the multiplicity, stability, and oscillatory dynamics of the non-adiabatic tubular reactor with a single $A \rightarrow B$ reaction. The techniques illustrate the existence of one, three, five, or seven steady states and bifurcating periodic solutions. We present numerical procedures for computing the Hopf bifurcation formulas which can determine the stability and location of the oscillation without integrating the parabolic partial differential equations. The combination of our Hopf techniques with steady state bifurcation methods enables us to determine all possible steady and stable oscillatory solutions exhibited by distributed parameter models such as the tubular reactor.

AMS(MOS) Subject Classification: 80A20, 35B10, 35B32

Key Words: Hopf bifurcation, chemical reactors, multiplicity, oscillations, stability

Work Unit No: 2 - Physical Mathematics

Sponsored by the United States Army under Contract No. DAAG29-80-C-0041.

SIGNIFICANCE AND EXPLANATION

Numerical methods are developed for the investigation of Hopf bifurcation (bifurcation to periodic solutions) in mathematical models which consist of parabolic partial differential equations whose time independent solutions are defined by systems of two point boundary value problems. The combination of our Hopf techniques with the steady state bifurcation methods of Keller enables us to determine all possible steady state and periodic solutions exhibited by these distributed parameter models. The utility of our numerical procedure lies in their generality and potential applicability. They can be used to study the multiplicity, stability, and oscillatory phenomena exhibited by reaction-diffusion systems in combustion, chemical reactor theory and mathematical biology.

We apply these techniques to a model of the tubular reactor with an exothermic reaction. The reactor is found to exhibit broad regions of multiple steady states and periodic solutions which can be conveniently presented on response curves to illustrate the dynamic capabilities of this reactor. We discuss the effects of the solutions on reactor operation, and the effects of sharp transitions or jumps between the steady states and oscillatory states on reactor dynamics. Many of the above results have not been reported in the earlier studies of the tubular reactor or in the more exhaustive studies of the continuously stirred tank reactor.

NUMERICAL HOPF BIFURCATION TECHNIQUES AND THE DYNAMICS OF THE TUBULAR REACTOR MODEL

Robert F. Heinemann and Aubrey B. Poore

INTRODUCTION

The number of theoretical and experimental investigations of multiplicity, stability, and sensitivity of reaction-diffusion systems over the past two decades has been enormous. Much of this research has centered around heat and mass transfer coupled with chemical reaction and has generally been motivated by the design and operation of industrial chemical reactors. The most widely studied reactor type has been the continuously stirred tank reactor (CSTR) since the relevant mathematics are comparatively tractable, and studies of the CSTR provide a foundation for the understanding of more complex reactors. Poore [1] and Uppal et al. [2,3] have presented an important and thorough consideration of the single, first-order exothermic reaction in the CSTR. They concisely classified all possible patterns of multiple steady and periodic states and pieced together a myriad of results presented in earlier papers. The Hopf bifurcation techniques presented by Poore and Uppal et al. were completely general for time-dependent ordinary differential equations and have been applied to other systems exhibiting oscillatory phenomena [4]. Such systems included those whose mathematical models consist of parabolic partial differential equations which can be judiciously simplified to ordinary differential equations [5]. These simplifications have been advantageous since Hopf bifurcation techniques were not available for distributed parameter models. The major objective of the present work is to fill this void by presenting the Hopf formulas for these complex systems.

Our numerical techniques are based entirely on the time-independent problem and yield the relevent bifurcation information such as the direction and stability of the oscillatory solution. Furthermore, the periodic orbit

Sponsored by the United States Army under Contract No. DAAG29-80-C-0041.

can be computed without time integration from an asymptotic formula for the orbit. These methods are quite general and can be applied to systems of parabolic partial differential equations whose time-independent solutions are defined by a two-point boundary value problem.

We illustrate the utility of our numerical techniques by applying them to the model of the nonadiabatic tubular reactor. Because of its fundamental importance, this reactor has been studied with only slightly less fervor than the CSTR. The formidable body of literature concerned with the problem includes the extensive work of Amundson et al. [5 - 15], Hlavecek et al. [16 - 19], and McGowin and Perlmutter [20]. Many of the results presented in these works are summarized and explained in two excellent reviews by Schmitz [21] and Varma and Aris [22]. These earlier papers have firmly established the existence of one, three, or five steady states and also have illustrated sustained oscillations. However, a complete understanding of the oscillatory dynamics is still largely an untouched problem.

Two recent papers concerning the multiplicity of the nonadiabatic tubular reactor should be mentioned at this point. Kapilla and Poore [23] have completely classified the structure of the multiple steady states for all possible parameters using large activation energy asymptotics and have established the existence of two additional solutions not seen in previous works. We [24] have confirmed and extended this classification by applying the steady state bifurcation techniques of Keller to the problem [25]. The effect of a wide range of finite activation energies has been examined and has shown the existence of one, three, five and seven solutions. Following presentation of the mathematical model of the reactor and our numerical procedures, we illustrate Hopf bifurcation results for multiplicity patterns exhibiting from one to seven steady states.

MATHEMATICAL MODEL

The equations describing the conservation of reactant A and energy for the nonadiabatic tubular reactor with axial mixing appear below in dimensionless form:

$$\frac{\partial y}{\partial \tau} = \frac{1}{Pe_m}\frac{\partial^2 y}{\partial s^2} - \frac{\partial y}{\partial s} - Dy\, e^{\gamma - \gamma/\theta} \tag{1}$$

$$\frac{\partial \theta}{\partial \tau} = \frac{1}{Pe_h}\frac{\partial^2 \theta}{\partial s^2} - \frac{\partial \theta}{\partial s} - \beta\,(\theta - \theta_0) + B\,Dy\, e^{\gamma - \gamma/\theta}\ . \tag{2}$$

The boundary and initial conditions are:

$$\frac{\partial y}{\partial s} = Pe_m(y-1) \qquad \text{at} \quad s = 0\ , \quad \tau > 0$$

$$\tag{3}$$

$$\frac{\partial \theta}{\partial s} = Pe_h(\theta - 1) \qquad \text{at} \quad s = 0\ , \quad \tau > 0$$

$$\frac{\partial y}{\partial s} = \frac{\partial \theta}{\partial s} = 0 \qquad \text{at} \quad s = 1\ , \quad \tau > 0 \tag{4}$$

$$y = y_{in}\ , \qquad \theta = \theta_{in} \quad \text{at} \quad \tau = 0\ . \tag{5}$$

In writing these equations, we have defined the following dimensionless quantities,

$$y = c/c_0 \qquad \theta = T/T_0$$

$$s = x/L \qquad \tau = tv/L$$

$$Pe_m = vL/D_e \qquad Pe_h = \rho C_p vL/k_e$$

$$B = \Delta Hc_0/\rho C_p T_0 \qquad \beta = UPL/av\rho C_p$$

$$D = Ae^{-\gamma}L/v \qquad \gamma = E/RT_0\ .$$

The above model describes an exothermic $A \rightarrow B$ reaction occurring in a homogeneous tube under the assumptions that the velocity profile is flat with constant velocity v; the variables y and θ depend only on one space dimension and time; the diffusion of reactant A is governed by Fick's Law with an effective diffusivity, D_e; heat conduction is described by Fourier's Law with an effective

thermal conductivity, k_e ; the heat loss at any point is proportional to $(\theta - \theta_0)$; and the reaction rate is describable by an Arrhenius expression.

The dimensional predecessors of the above equations and the applicability of this formulation are discussed in detail in the two review articles and in the earlier reactor papers.

NUMERICAL METHODS

We now present the numerical techniques for generating the steady state response curves and the Hopf bifurcation information for systems whose mathematical description is given by a distributed parameter model. The coupling of these methods enables us to systematically locate all the possible steady and periodic states exhibited by these systems. We begin with a discussion of the general forms of the equations that we are capable of treating.

Many of the distributed parameter models in chemical reactor theory can be written as a system of parabolic partial differential equations of the form

$$\begin{aligned} &\frac{\partial u}{\partial t} = A(\mu)\,\frac{\partial^2 u}{\partial x^2} + f(u,\, u_x,\, \mu) \\ &G_\ell(u(a),\, u_x(a), \mu) = 0 \\ &G_r(u(b),\, u_x(b), \mu) = 0 \end{aligned} \tag{6}$$

where u may represent, for example, the concentration and temperature in the reactor. G_ℓ and G_r denote the left and right boundary conditions (possibly nonlinear) and μ is the bifurcation parameter. The function f may depend nonlinearly on u, u_x, and μ and may contain the space variable x explicitly but not the time variable t. For brevity we write this system as

$$\frac{du}{dt} = F(u,\mu)\ , \qquad G(u,\mu) = 0\ . \tag{7}$$

The corresponding two-point boundary value problem is denoted by

$$F(v,\mu) = 0\ , \qquad G(v,\mu) = 0\ . \tag{8}$$

Steady State Numerical Techniques

The steady state problem (8) was solved by combining Keller's modification of the Euler-Newton continuation method [25] with de Boor and Wiess' spline collocation code [26] and a fourth-order finite difference scheme due to Stepleman [27]. Both the collocation and finite difference methods performed quite well with the collocation technique capable of higher accuracy.

The objective of the steady state methods is to compute the solution v of equation (8) as the parameter μ assumes all its possible values. The

Euler-Newton continuation method can be used to solve this problem with Euler's method (9) serving as a predictor for Newton's method (10)

$$v^0(\mu + \delta\mu) = v(\mu) + \delta\mu \frac{du(\mu)}{d\mu} \tag{9}$$

$$v^{i+1}(\mu+\delta\mu) = v^i(\mu+\delta\mu) - F_v^{-1}(v^i(\mu+\delta\mu),\mu+\delta\mu)F(v^i(\mu+\delta\mu),\mu+\delta\mu). \tag{10}$$

However, the technique fails near transition between steady states since the Jacobian matrix, F_v, cannot be inverted near singularities such as limit or bifurcation points.

Keller has modified the above method by imposing an additional normalization on the solution which enables entire solution branches to be traced, skipping over any singular points. The imposition of this constraint allows the specification of a new parameter, s, which replaces μ as the continuation parameter in the Euler-Newton technique. The reparameterized problem becomes

$$P(x,s) = 0 \tag{11}$$

where

$$x(s) = (v(s),\mu(s)) \tag{12}$$

and

$$P(x(s),s) = \begin{Bmatrix} F(v(s), \mu(s)) \\ N(v(s), \mu(s),s) \end{Bmatrix}$$

It is convenient to choose the normalization $N(v,\mu,s)$ so that s approximates the arc-length of the solution branch for some parameter $\alpha \in (0,1)$

$$N(v,\mu,s) = \alpha\|v(s) - v(s_0)\|^2 + (1-\alpha)|\mu(s) - \mu(s_0)|^2 - (s - s_0)^2. \tag{13}$$

When the Euler-Newton technique is applied to (11), computational difficulties near singularities are eliminated since the Jacobian matrix remains nonsingular near such points.

These techniques and an algorithm for their implementation are presented in detail by Keller [25] and have previously been applied to laminar flame problems

[28-30] and catalysts problems [31] which exhibit multiple steady states. Therefore, we forego a discussion of the exact computational procedure.

Hopf Bifurcation Formalism

We use the term formalism here since the presentation will be stripped of the technical mathematical assumptions. A proper mathematical framework can be found in the works of Crandall and Rabinowitz [32] and Ioos and Joseph [33]. Our work follows closely the presentation in the latter paper, though modified somewhat to account for the nonzero steady state problem and the form of the model equations (7). Since this bifurcation theory is most effectively used in a study of the dynamics associated with an exchange of stability, we begin with a brief discussion of steady state stability.

The stability of time-independent solutions can in principle be resolved by examining the eigenvalues of the linearized boundary value problem. If the eigenvalues all have negative real parts, the steady state is stable; whereas, if an eigenvalue has a positive real part, the solution is unstable. Exceptions to this principle occur when the linearized problem has a zero eigenvalue or a pair of complex conjugate, purely imaginary eigenvalues. In the current reactor problem, a zero eigenvalue gives rise to a limit point bifurcation (a point of vertical tangency) on the response curves. The bifurcation of a periodic solution (Hopf bifurcation) occurs when a pair of complex conjugate eigenvalues $\sigma(\mu)$ and $\bar{\sigma}(\mu)$ become purely imaginary. We assume that this crossing of the imaginary axis occurs at μ_0 so that $\sigma(\mu_0) = +i\omega_0$ with ω_0 positive. It is also assumed that $\mathrm{Re}\ \sigma_\mu(\mu_0) \neq 0$ where $\sigma_\mu = d\sigma/d\mu$. This ensures a strict crossing of the axis and is nearly always satisfied in these problems.

When the Hopf point is accompanied by an exchange of stability, different types of periodic phenomena may be encountered. If the periodic orbit is stable, a small amplitude oscillation is observed near the Hopf point, but if the orbit is unstable, the solution will jump to either a large amplitude, stable oscillation or to another stable steady state. Examination of the orbit stability near the Hopf points suggests a systematic procedure for locating the stable oscillations in the reactor.

To present the Hopf bifurcation formulas, we linearize the boundary value problem and write it as

$$L_\mu w = 0 , \qquad G_v(v^\mu,\mu|w) = 0 \tag{14}$$

where

$$L_\mu w = F_v(v^\mu,\mu|w) = \frac{\partial}{\partial\delta} F(v^\mu + \delta w,\mu)\Big|_{\delta=0}$$

and

$$G_v(v^\mu,\mu|w) = \frac{\partial}{\partial\delta} G(v^\mu + \delta w,\mu)\Big|_{\delta=0} .$$

The essential requirements for Hopf bifurcation without their technical assumptions may be summarized as follows. Assume $\pm i\omega_0$ are simple eigenvalues of L_{μ_0}, that $ni\omega_0$ is not an eigenvalue for $n = 0,2,3,\ldots,$ and that the real part of $\sigma_\mu(\mu_0)$ is nonzero. Then one can construct a bifurcating periodic solution of (7) with frequency $\omega(\varepsilon)$ via a perturbational expansion which can be shown to take the form [34]

$$u(x,t) = v^{\mu_0} + 2\,\varepsilon\,\mathrm{Re}\{\zeta_0\, e^{is}\} + \frac{\varepsilon^2}{2}\{w_1 + \mu_2 \frac{dv^{\mu_0}}{d\mu} + 2\,\mathrm{Re}\{w_2 e^{2is}\}\} + O(\varepsilon^2) \tag{15}$$

$$\mu = \mu_0 + \frac{\varepsilon^2}{2}\mu_2 + O(\varepsilon^2) \tag{16}$$

$$w(\varepsilon) = \omega_0 + \frac{\varepsilon^2}{2}\omega_2 + O(\varepsilon^2) \tag{17}$$

$$t = \omega(\varepsilon)s \tag{18}$$

ε is an auxiliary parameter representing the amplitude of the orbit close to the Hopf point. The vector function ζ_0 is the eigenvector corresponding to the eigenvalue $+i\omega_0$; w_1 and w_2 are solutions of certain linear nonhomogeneous boundary value problems discussed in the next section. We note that the sign of μ_2 yields the sign of $\mu - \mu_0$ for ε sufficiently small and therefore determines the direction of bifurcation. Similarly, ν_2 determines the change in the frequency of the bifurcating solution. The perturbational expansion (15) provides a good approximation to the periodic solution for computational purposes.

The stability of the bifurcating oscillation can be based on a study of the Floquet exponents as discussed by Iooss and Joseph [34]. The essential result is that the periodic solution will be locally stable near the bifurcation point if the eigenvalues of L_{μ_0}, other than $\pm i\omega_0$, have negative real parts and if μ_2 Re $\sigma_\mu(\mu_0)$ is positive.

The relevant bifurcation information can be extracted if μ_2, ν_2 and $\sigma_\mu(\mu_0)$ are computed. The algorithm for computing each of these is presented next.

An Algorithm for the Hopf Bifurcation Formulas.

The nonlinear two-point boundary value problem

$$F(v^\mu,\mu) = 0 , \quad G(v^\mu,\mu) = 0 \tag{19}$$

must first be solved at a point μ_0 where the linearized problem (14) has a pair of purely imaginary eigenvalues $\pm i\omega_0$. Thus, the Hopf point is located by finding a root μ_0 of Re $\sigma(\mu)$. This is accomplished by using the QZ algorithm to compute the eigenvalues at each point along the steady state response curves and then employing the bisection or secant method to locate μ_0.

Let $L^*_{\mu_0}$ denote the adjoint differential equation, and $G^*_v(v^{\mu_0},\mu_0|\cdot)$, the adjoint boundary conditions. The eigenvectors ζ_0 and ζ_0^* are then computed from the eigenvalue problems

$$L_{\mu_0}\,\zeta_0 = i\omega_0\,\zeta_0\ ,\quad G_v(v^{\mu_0},\mu_0|\zeta_0) = 0\ ; \tag{20}$$

$$L^*_{\mu_0}\,\zeta^*_0 = -i\omega_0\zeta^*_0\ ,\quad G^*_v(v^{\mu_0},\mu_0|\zeta^*_0) = 0\ . \tag{21}$$

These eigenvectors are then normalized by requiring

$$\langle\,\zeta_0,\,\zeta_0\,\rangle = 1 \quad \text{and} \quad \langle\,\zeta_0,\,\zeta^*_0\,\rangle = 1\ . \tag{22}$$

Here we have introduced the complex L_2 inner product

$$\langle\,\psi,\phi\,\rangle = \int_a^b \psi\cdot\bar{\phi}\,dx \tag{23}$$

where $\psi\cdot\bar{\phi}$ denotes the dot product of the vector functions ψ and ϕ.

A sequence of three linear nonhomogeneous boundary value problems must next be solved. These are

$$\begin{aligned} &L_{\mu_0}\frac{dv^{\mu_0}}{d\mu} = -F_\mu(v^{\mu_0},\mu_0)\\ &G_v(v^{\mu_0},\mu_0|\frac{dv^{\mu_0}}{d\mu}) = -G_\mu(v^{\mu_0},\mu_0) \end{aligned} \tag{24}$$

$$\begin{aligned} &L_{\mu_0}w_1 = -2F_{vv}(v^{\mu_0},\mu_0|\zeta_0,\bar{\zeta}_0)\\ &G_v(v^{\mu_0},\mu_0|w_1) = -2G_{vv}(v^{\mu_0},\mu_0|\zeta_0,\bar{\zeta}_0) \end{aligned} \tag{25}$$

$$\begin{aligned} &(L_{\mu_0} - 2i\omega_0 I)w_2 = -F_{vv}(v^{\mu_0},\mu_0|\zeta_0,\zeta_0)\\ &G_v(v^{\mu_0},\mu_0|w_2) = -G_{vv}(v^{\mu_0},\mu_0|\zeta_0,\zeta_0)\ . \end{aligned} \tag{26}$$

The derivatives F_{vv} and G_{vv} appearing in the above problems are computed by the rule

$$F_{vv}(v^\mu,\mu|\phi,\psi) = \frac{\partial^2 F}{\partial\delta_1\partial\delta_2}(v^\mu + \delta_1\phi + \delta_2\psi,\mu)\Big|_{\delta_1=\delta_2=0}\ . \tag{27}$$

With these computations complete, we now compute $\sigma_\mu(\mu_0)$, μ_2, and ω_2 from

$$\sigma_\mu(\mu_0) = \langle F_{vv}(v^{\mu_0},\mu_0|\zeta_0,\frac{dv^{\mu_0}}{d\mu}) + F_{v\mu}(v^{\mu_0},\mu_0|\zeta_0),\zeta^*_0\,\rangle \tag{28}$$

and

$$\{-i\omega_2 + \mu_2\sigma_\mu(\mu_0)\} = -\langle F_{vvv}(v^{\mu_0},\mu_0|\zeta_0,\zeta_0,\bar{\zeta}_0),\zeta_0^*\rangle$$
$$-\langle F_{vv}(v^{\mu_0},\mu_0|\zeta_0,w_1),\zeta_0^*\rangle \qquad (29)$$
$$-\langle F_{vv}(v^{\mu_0},\mu_0|\bar{\zeta}_0,w_2),\zeta_0^*\rangle \ .$$

The first author evaluated the above expressions by using the Stepleman finite difference scheme to solve equations (24-26) and using Simpson's rule to numerically integrate the inner products. The second author solved the boundary value problems with the de Boor and Weiss' collocation code and integrated the inner products via Gauss-Lobatto quadrature. Both methods worked well and yielded quite comparable results for $\sigma_\mu(\mu_0)$, μ_2 and ω_2. (A program for the Hopf computations for the general problem (6) will be available from the second author.)

We note that for computations where numerical sensitivity was observed, the sensitivity could be eliminated by more accurate computations of the steady state solution v^{μ_0}, the eigenvectors ζ_0 and ζ_0^*, and the parameter value μ_0 at which $\mathrm{Re}\ \sigma(\mu_0) = 0$. This sensitivity is not removed by increasing the accuracy of the μ_0 calculation for a specific discretization as in the case for ordinary differential equations. Some obvious tests for accuracy are an orthogonality relation for ζ_0 and ζ_0^*, $\langle \zeta_0,\bar{\zeta}_0^*\rangle = 0$; the size of $\mathrm{Re}\ \sigma(\mu_0)$; and perhaps more importantly, comparisons of the eigenvalues of the linearized problem (14) and its adjoint.

RESPONSE CURVES

In this section, we present some of the more interesting results obtained by using the above numerical techniques to study the dynamics of the tubular reactor which arise from varying the Damköhler number. It is to be emphasized that this is not a complete cataloging of the dynamic capabilities of the reactor but rather a presentation of the more illustrative cases found in our investigations. Many of the response curves are not found in the CSTR studies and are thus somewhat unexpected. The cases that are presented can be viewed, in our opinion, as giving a much more complete picture of the interplay between the instabilities in the steady states and the oscillatory dynamics that can arise during operation of the reactor.

For a particular combination of the system parameters, we summarize the multiplicity and stability of the steady states and oscillatory states on a response curve with the Damköhler number as the abscissa and the maximum temperature of the steady state or periodic solution as the ordinate. The steady state solution branches are computed by using Keller's modification of the Euler-Newton procedure; the stability of these branches and the location of the bifurcation points are determined by an eigenvalue analysis. The Hopf bifurcation formulas (16-18) are then computed to give the direction of bifurcation and the stability of the bifurcating periodic solutions. By using the asymptotic formula (15) for the solution near the bifurcation point, we are able to start tracing the stable oscillations as the Damköhler number is varied by solving the full parabolic partial differential equations with PDECOL, a general code based on the method of lines and collocation using B-splines [34].

The first example is illustrated in Figure 1 which corresponds to the parameter values $P_{e_h} = P_{e_m} = 5$, $B = 0.5$, $\gamma = 25$, $\beta = 3.5$, and $\theta_0 = 1$. For all values of the Damköhler number, D, the steady state is unique with

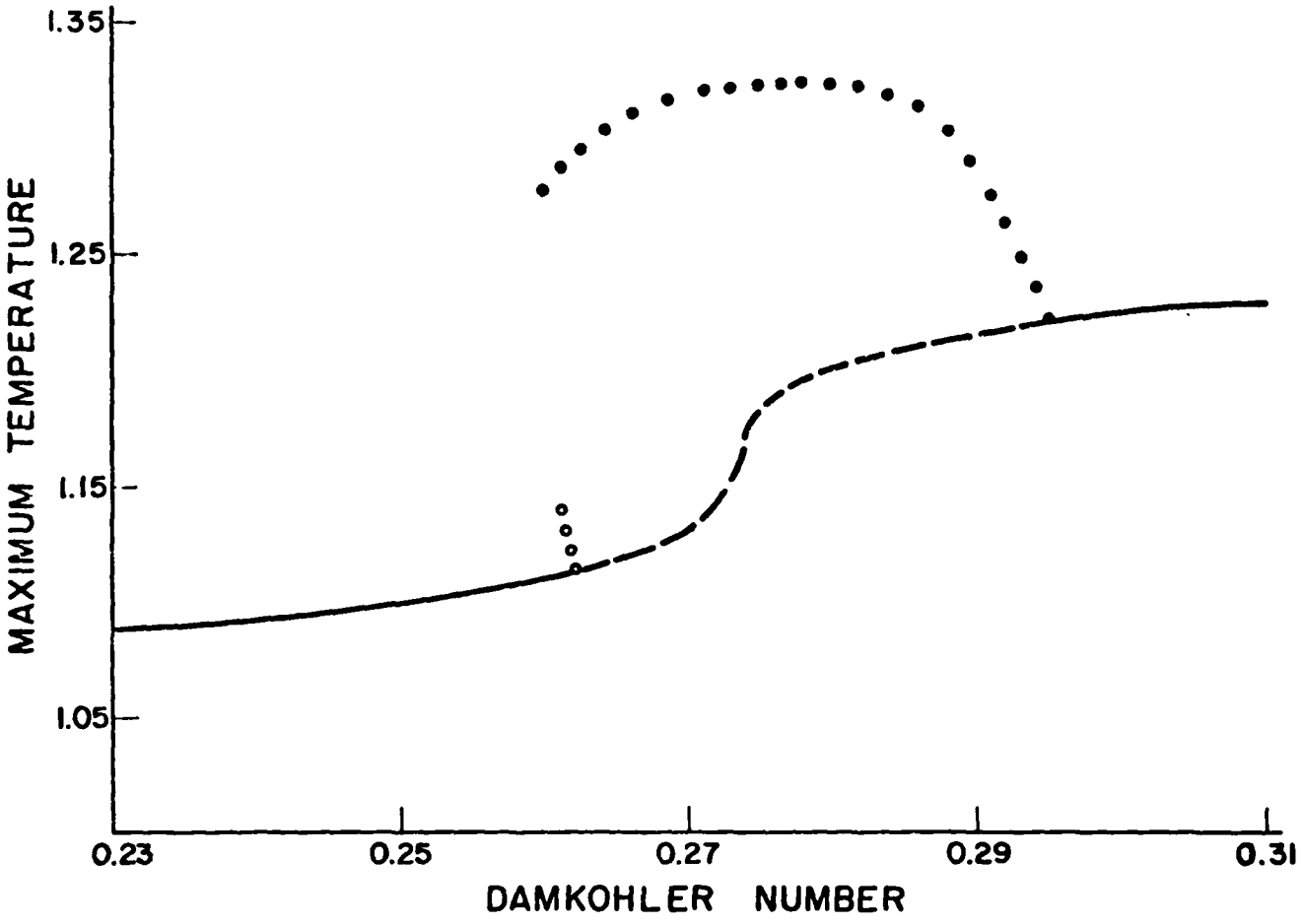

Figure 1. Bifurcation to Oscillatory States in the Nonadiabatic Tubular Reactor (Pe=5, B=0.50, γ=25, and β=3.5; —— stable steady states, ---- unstable steady states, ... stable periodic orbits, ∘∘∘∘ unstable periodic orbits)

exchanges instability at $D = 0.262$ and $D = 0.295$. At the value $D = 0.295$, stable periodic solutions bifurcate to the left, while at $D = 0.262$, the solutions also bifurcate to the left but are not stable. PDECOL was used to trace the stable oscillation from $D = 0.295$ down to $D = 0.260$ where the stable oscillations cease to exist and the time-dependent solutions converge to the stable steady state directly below. (We conjecture that the stable branch of periodic solutions connect with the unstable branch emanating from $D = 0.262$.)

The response curve dynamics associated with varying the Damköhler number can now be explained for the case depicted in Figure 1 . For D close to zero, the reactor operates in stable state of low temperature and low conversion of reactant A . As D is increased, the steady state remains stable and the steady state temperature rises slowly until D passes through $D = 0.262$. A jump occurs at this point in the temperature and concentration profiles into the stable oscillation directly above. These oscillatory solutions remain until D reaches $D = 0.295$ after which the reactor operates in a stable steady state. To lower the conversion and temperature in the reactor, the Damköhler number is now decreased. At $D = 0.295$ a small stable oscillation in the temperature and concentration profiles begins to appear. These oscillations continue until $D = 0.260$ at which point the oscillations disappear through a jump back down to the lower, stable steady state. Both of these jumps may be thought of as ignition or extinction processes, respectively.

In Figure 2, β is decreased to 2.5 and a region of three steady states appears. Exchanges of stability again occur at the Hopf points, and at the upper point ($D = 0.1818$), the behavior of the oscillation is similar to that of Figure 1. The stable periodic solution bifurcates to the left and its amplitude quickly increases. The orbit at the lower Hopf point ($D = 0.165$) bifurcates sharply upward to the right and is stable. The continuation of these stable branches is quite interesting. Attempts to continue the larger amplitude periodic branch below $D = 0.172$ failed with the time-dependent calculations converging to the lower

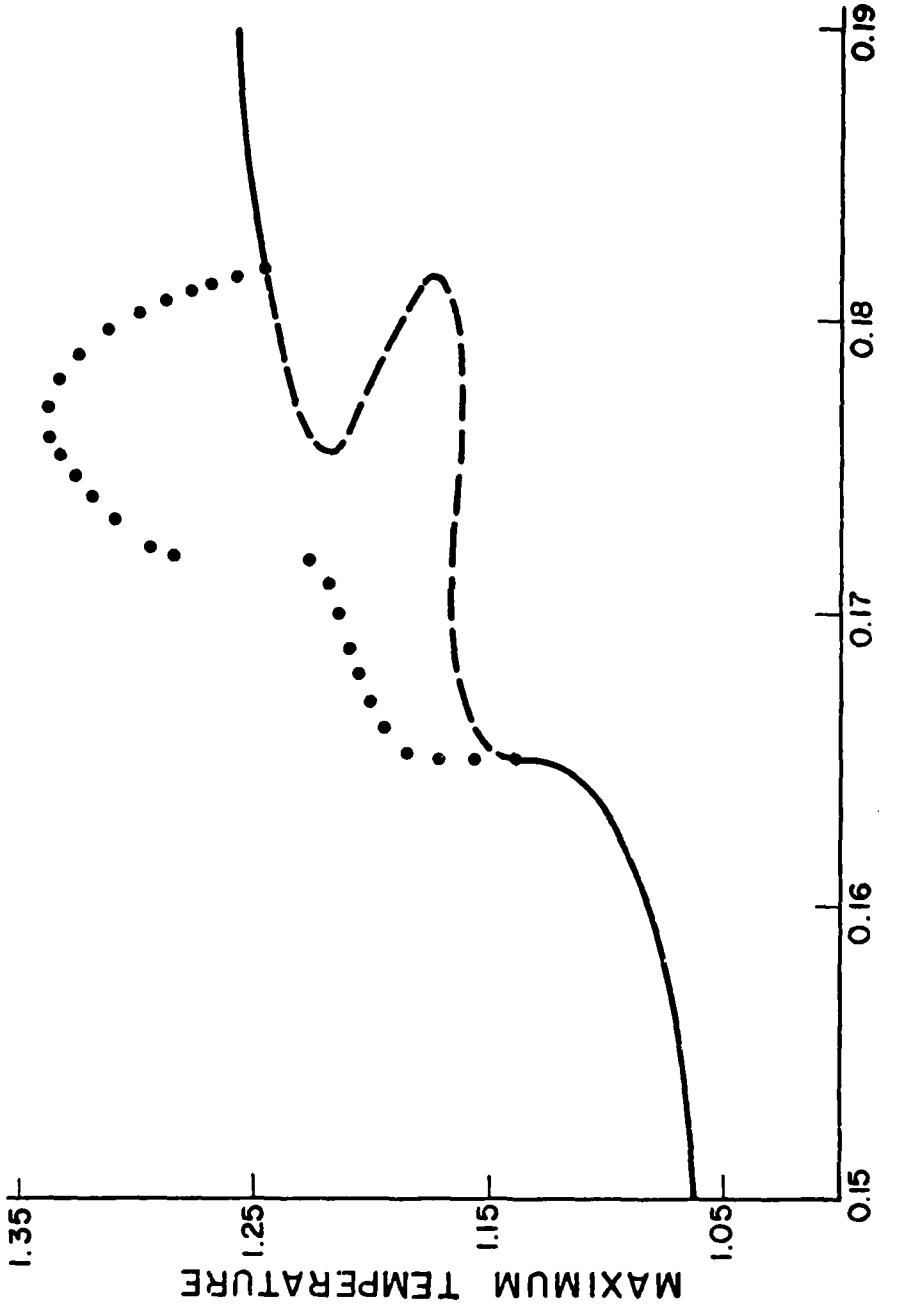

Figure 2. Existence of Stable Oscillatory Solutions Surrounding Multiple and Unique Steady States (Pe=5, B=0.50, γ=25, and β=2.5)

amplitude periodic solutions regardless of the initial conditions. When the unsteady-state calculations were started on the lower portion of the branch and D was increased above 0.172, the periodic orbit jumped to the upper solutions. The temperature profiles from the upper and lower periodic branches are presented in Figures 3 and 4. The explanation of this seemingly new jump phenomena along the periodic branch is the subject of current investigation. Since the response curve in this case is similiar to the curve in Figure 5 , we forego a discussion of the possible reactor dynamics for this case.

The dimensionless heat transfer coefficient is lowered to 2.35 in Figure 5 where 1-3-1-3-1 multiplicity arises. If D starts near zero and is increased, the reactor temperature increases and remains in a stable steady state until the lower limit point is encountered at which point the temperature jumps into the much higher stable oscillation. This stable oscillation surrounds the unstable steady states and grows steadily until a jump to an even higher stable oscillation occurs at about D = 0.159. The amplitude of the temperature oscillation continues to grow, peaks out, and then rapidly decays to the steady state at D = 0.166. The reactor can now be extinguished by decreasing the Damköhler number. The amplitude of the periodic orbits bifurcating at D = 0.166 grows rapidly, peaks out, decays, jumps down, continues to decay, and then disappears as the time-dependent solutions converge to the lower, stable steady states beginning at the lower turning point. (It should be pointed for this case that the frequency of the oscillation decreases along the lower periodic branch as D is decreased. The period of the oscillatory solution above the lower limit point is approximately five times greater than the period of the orbit of the Hopf point, D = 0.166.)

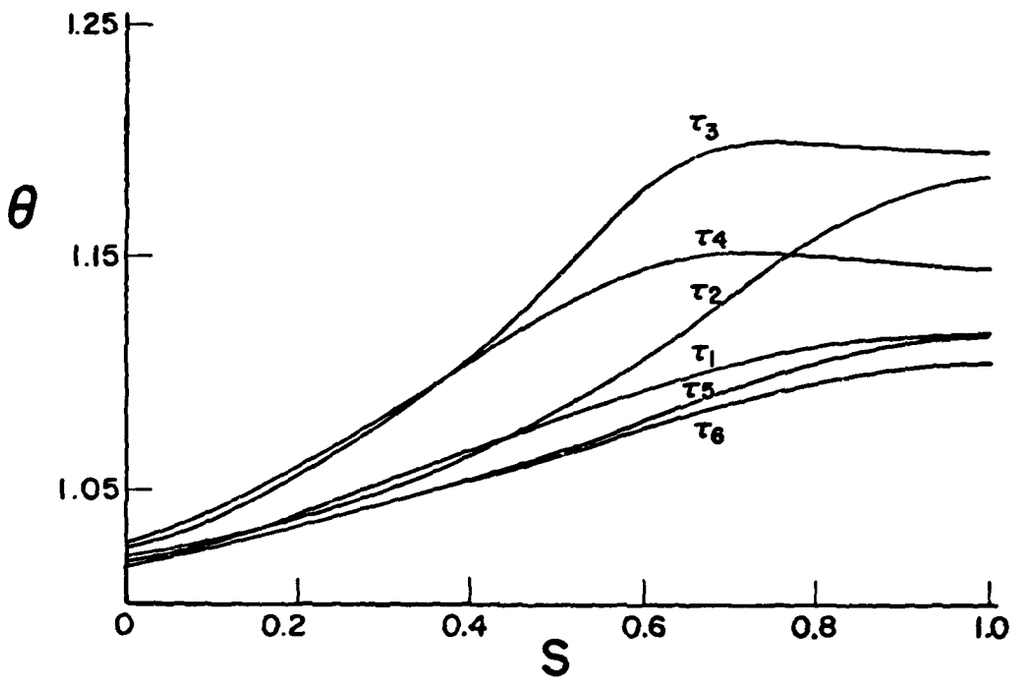

Figure 3. Time Variation of the Reactor Temperature Profile During One Period of Oscillation (Pe=5, B=0.50, γ=25, β=2.5, and D=0.170)

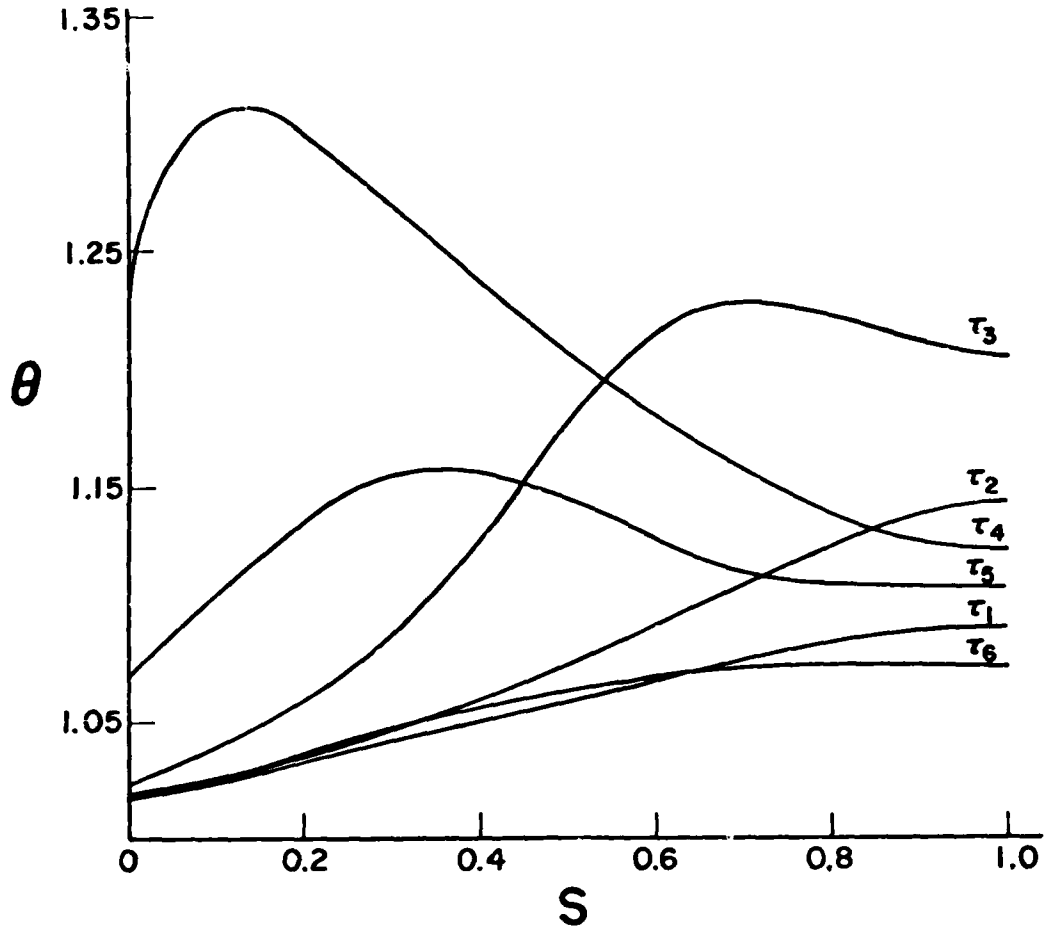

Figure 4. Time Variation of the Reactor Temperature Profile During One Period of Oscillation (Pe=5, B=0.50, γ=25, β=2.5 and D=0.170)

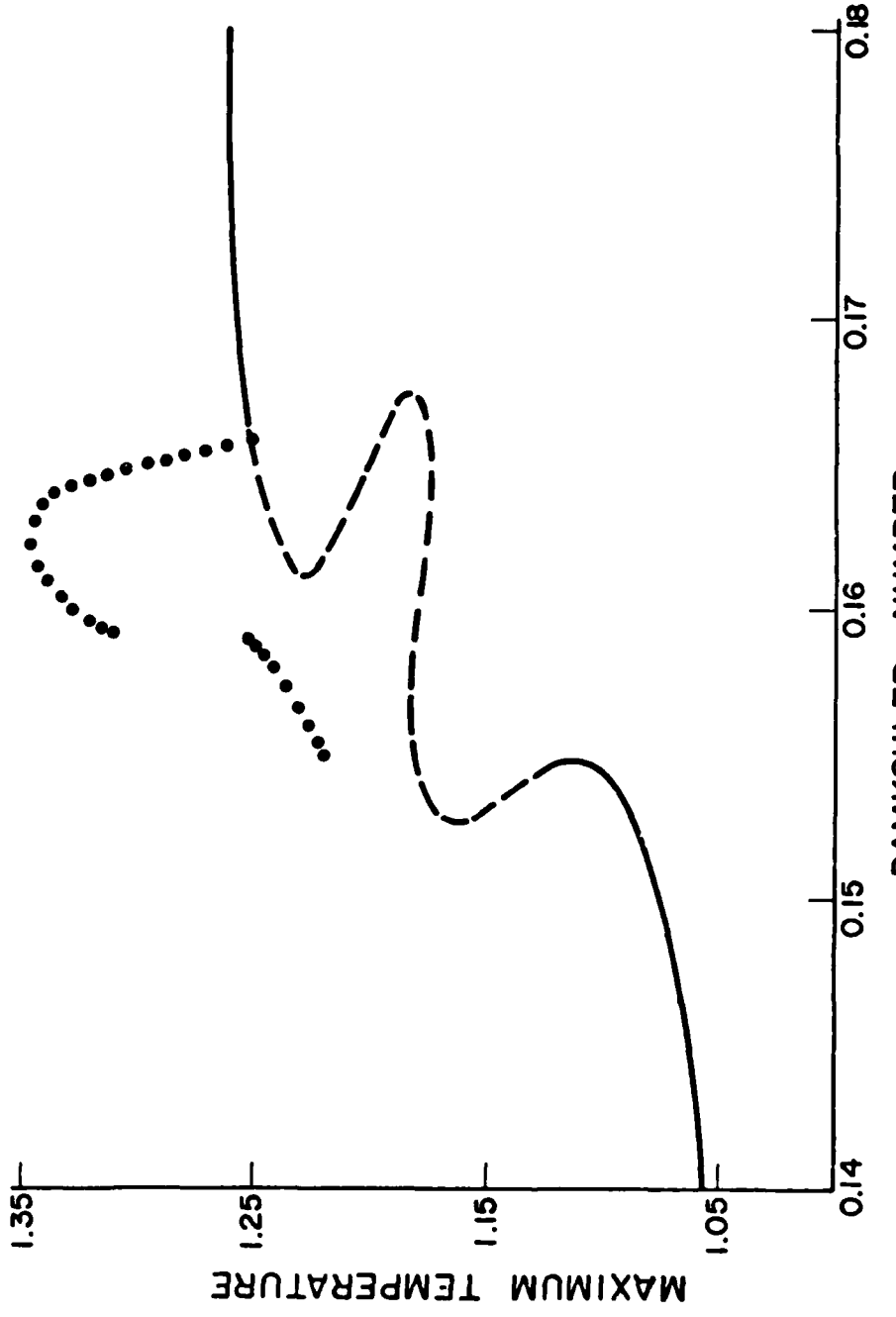

Figure 5. Existence of Stable Oscillatory Solutions Surrounding Multiple and Unique Steady States (Pe=5, B=0.50, γ=25, and β=2.35)

The existence of five steady states for the reactor is shown in Figure 6 where β is decreased to 2 . A Hopf point is located along the upper section of the steady state branch, and an unstable, periodic orbit bifurcates to the right of this point. While it is conceivable that a turning point could join this unstable branch with a stable one, time-dependent calculations did not locate any stable period solutions in this example. Furthermore, ω_2 (which governs the asymptotic change in frequency) is a large negative number and indicates the period of the unstable solution becomes infinite near the Hopf point.

It is a straightforward procedure to trace the bifurcation diagrams for $\beta = 1$ and $\beta = 0$ to complete this series of examples. However, Hopf bifurcation does not appear for these cases. For $\beta = 1$, the reactor exhibits five steady states with an exchange of stability at each limit point and the well-known adiabatic result of three steady states is found when $\beta = 0$.

In the last two figures, we show periodic solutions bifurcating from new patterns of multiple steady states [24]. Five steady states are illustrated in Figure 7 (Pe = 1, B = 0.50, γ = 75, and β = 4), and we note the existence of three Hopf points. The periodic solutions bifurcating to the right and to the left from the intermediate steady states are unstable, because an exchange of steady state stability does not accompany the bifurcation. The solutions at the upper Hopf point bifurcate to the left, are stable, but become infinitely periodic very near the bifurcation point.

The reactor model exhibits one, three, five, and seven steady states as well as bifurcating periodic solutions in Figure 8 (Pe=1, B=0.50, γ=125, and β=4). Both of the periodic orbits bifurcate to the left and both become infinitely periodic near the Hopf point. Only the periodic solutions bifurcating just to the right of the upper quench point are stable.

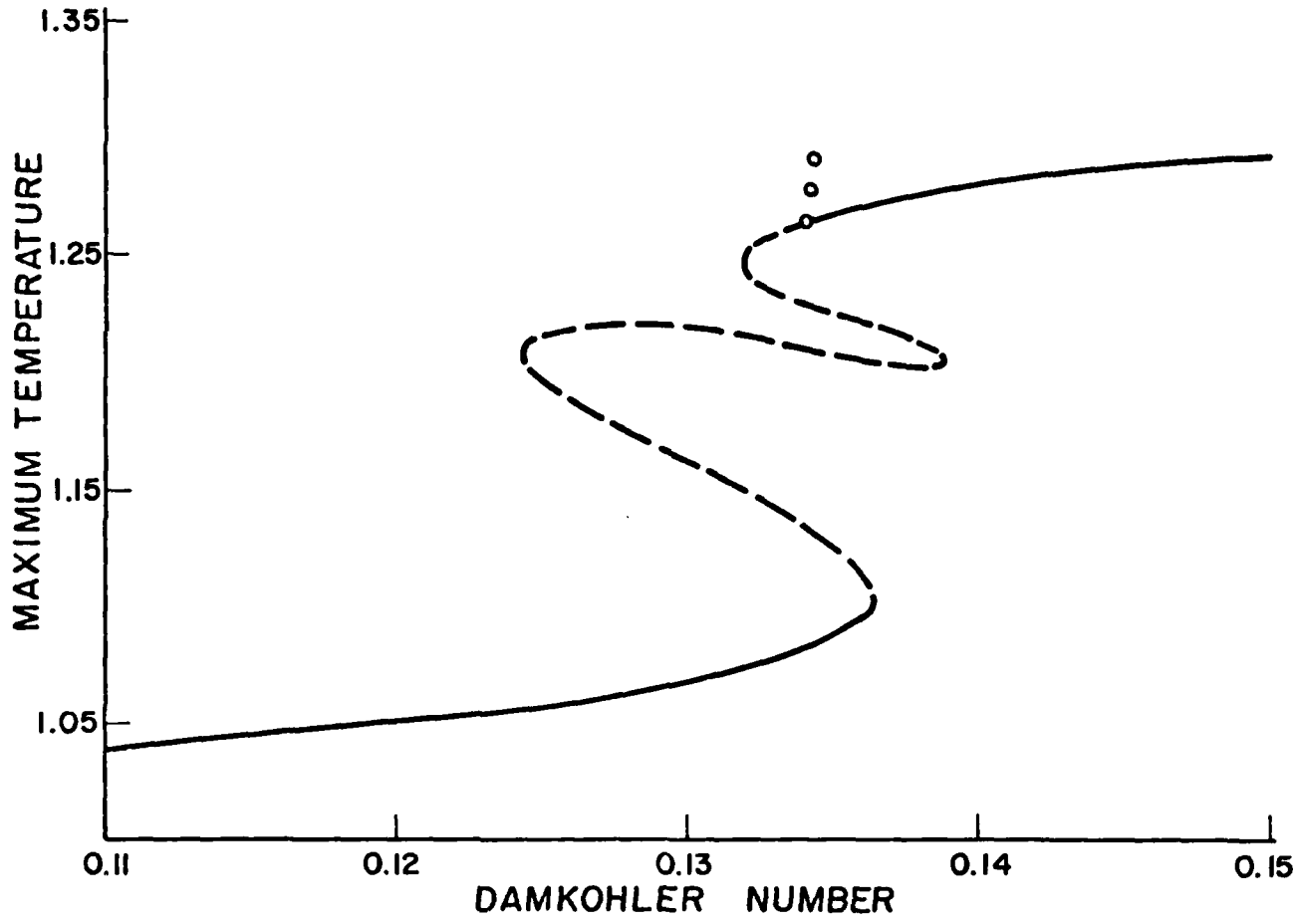

Figure 6. Existence of Unstable Bifurcation and Five Steady States (Pe=5, B=0.50, γ=25, and β=2)

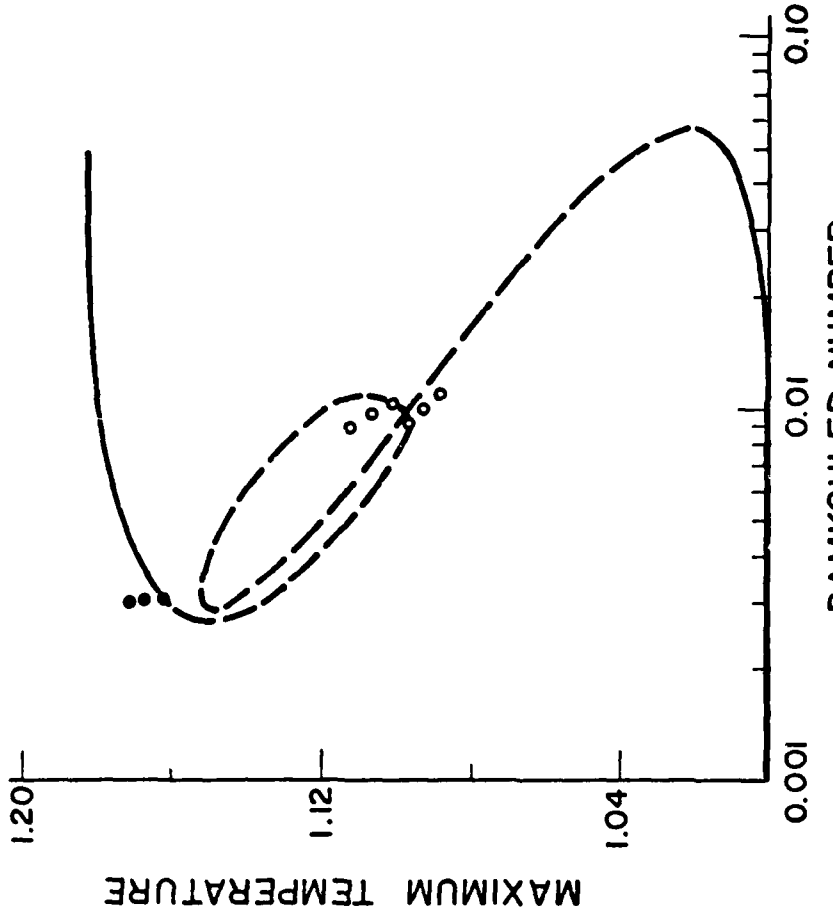

Figure 7. Multiple Bifurcating Orbits and Five Steady States (Pe=1, B=0.50, γ=75 and β= 4)

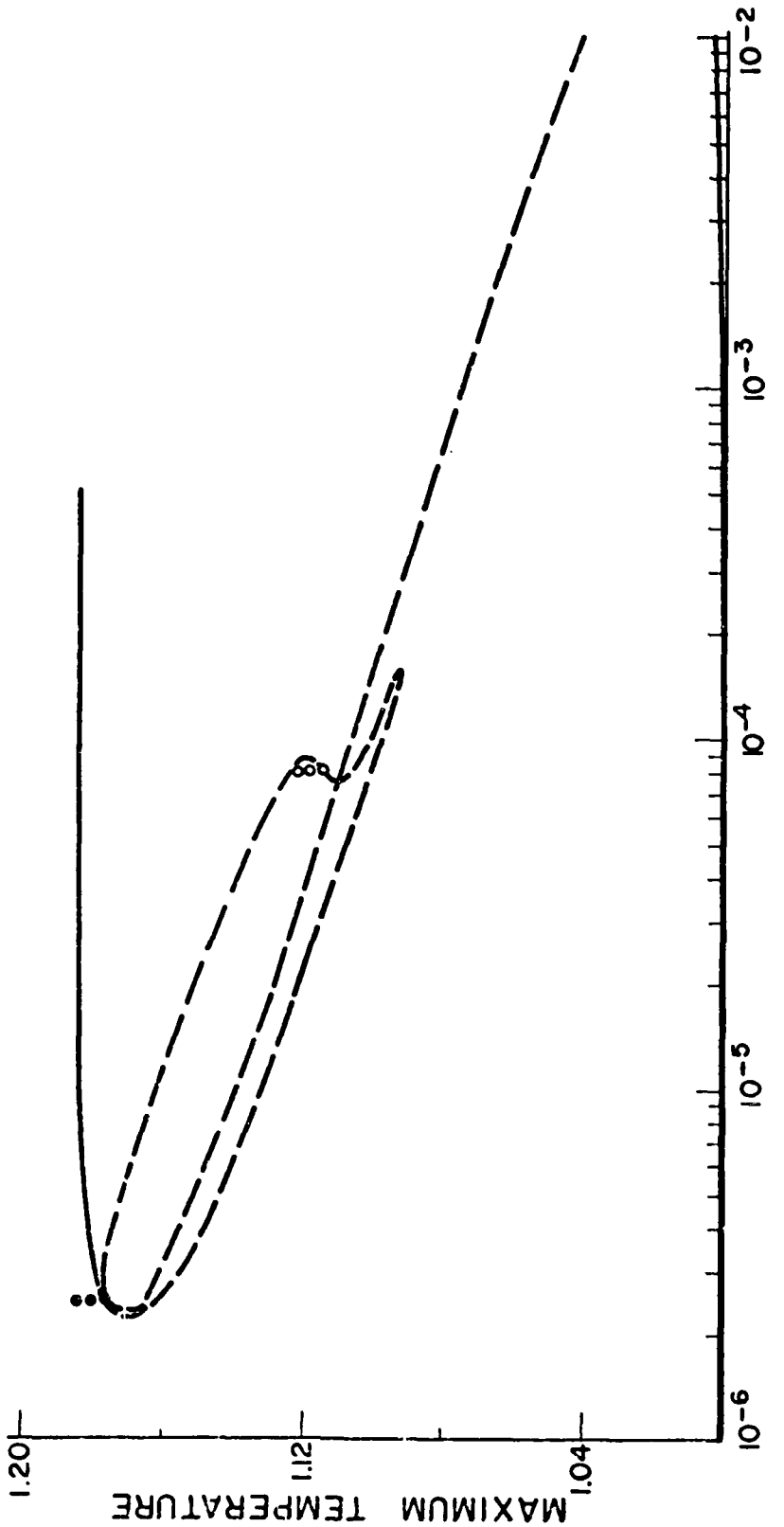

Figure 8. Existence of Multiple Periodic Solutions and Seven Steady States (Pe=1, B=0.50, γ=125, and β=4)

In Figures 6-8, the response curves become quite complex exhibiting several steady states and oscillatory solutions. However, the dynamic capabilities of the reactor in these examples are somewhat limited since many of the states are unstable over a large range of the Damköhler number. Ingition is characterized by increasing D past a lower limit point so that the reactor jumps from a stable, low temperature steady state to a stable, high temperature steady state. The reactor is extinguished by decreasing D until a jump occurs from an upper stable state (either a steady state or a periodic state with small amplitude) down to a lower, stable steady state. In these last three examples, jumps from lower steady states to large amplitude periodic solutions, jumps between oscillatory states, and possible periodic reactor operation over large regions of the Damköhler number are not possible.

CONCLUSIONS

We have presented numerical bifurcation techniques which can determine all possible steady and stable oscillatory solutions exhibited by distributed parameter models. These techniques were applied to the nonadiabatic tubular reactor and illustrated several types of steady state and oscillatory phenomena. Many of the results were anticipated from studies of the CSTR, but it is clear that all the possible phenomena exhibited by the tubular reactor has not been uncovered. The effects of parameters such as the feed temperature and flow velocity which could be used to control the reactor are largely unknown. With the proper motivation and support, our techniques can be used to solve these problems. Furthermore, because of their generality, these numerical methods can also be applied to a broad array of models found in combustion theory and mathematical biology as well as in chemical reactor theory.

REFERENCES

1. Poore, A. B., Arch. Rational Mech. Anal. 1973 52 358.
2. Uppal, A., Ray, W. H. and Poore, A. B., Chem. Engng. Sci. 1974 29 967.
3. Uppal, A., Ray, W. H. and Poore, A. B., Chem. Engng. Sci. 1976 37 205.
4. Poore, A. B., Math. Bios. 1975 26 99.
5. Ray, W. H., Uppal, A. and Poore, A. B., Chem. Engng. Sci. 1974 29 1330.
6. Raymond, L. R. and Amundson, N. R., Can. J. Chem. Engng. 1964 42 173.
7. Amundson, N. R., Can. J. Chem. Engng. 1965 43 49.
8. Luss, D. and Amundson, N. R., Chem. Engng. Sci. 1967 22 253.
9. Luss, D. and Amundson, N. R., Can. J. Chem. Engng. 1967 45 341.
10. Luss, D. and Amundson, N. R., Can. J. Chem. Engng. 1968 46 424.
11. Varma, A. and Amundson, N. R., Chem. Engng. Sci. 1972 27 907.
12. Varma, A. and Amundson, N. R., Can. J. Chem. Engng. 1972 50 470.
13. Varma, A. and Amundson, N. R., Can. J. Chem. Engng. 1973 51 206.
14. Varma, A. and Amundson, N. R., Can. J. Chem. Engng. 1973 51 459.
15. Amundson, N. R., SIAM - AMS Proc. 1974 8 59.
16. Hlavecek, V. and Hoffmann, H., Chem. Engng. Sci. 1970 25 173.
17. Hlavacek, V. and Hoffmann, H., Chem. Engng. Sci. 1970 25 187.
18. Hlavecek, V. and Hoffmann, H., Chem. Engng. Sci. 1970 25 1517.
19. Hlavacek, V., Hoffmann, H. and Kubecek, M., Chem. Engng. Sci. 1971 26 1629.
20. McGowen, C. R. and Perlmutter, D. D., A.I. Ch. E. J. 1971 17 831.
21. Schmitz, R. A., Adv. Chem. Ser. 1975 148 156.
22. Varma, A. and Aris, R., In Chemical Reactor Theory (Edited by L. Lapidus and N. R. Amundson), p. 79. Prentice-Hall, Englewood Cliffs, N. J. 1977.
23. Kapilla, A. K. and Poore, A. B., Submitted for publication, 1980.
24. Heinemann, R. F. and Poore, A. B., Submitted for publication, 1980.

25. Keller, H. B., In Applications of Bifurcation Theory (Edited by P. H. Rabinowitz), p. 359. Academic Press, New York 1977.

26. de Boor, C. and Weiss, R., MRC Tech. Summary Rep. #1625, University of Wisconsin, Madison, Wisconsin 1976.

27. Stepleman, R. S., Math. Comp. 1976 30 92.

28. Heinemann, R. F., Overholser, K. A. and Reddien, G. W., Chem. Engng. Sci. 1979 34 833.

29. Heinemann, R. F., Overholser, K. A. and Reddien, G. W., A. I. Ch. E. J. in press 1980.

30. Peterson, J. Overholser, K. A. and Heinemann, R. F., Chem. Engng. Sci. in press 1980.

31. Bissett, E. and Cavendish, J. C., 72nd Annual A. I. Ch. E. Meeting San Francisco 1979.

32. Crandall, M. G. and Rabinowitz, P. H., MRC Tech. Summary Rep. #1604, University of Wisconsin, Madison, Wisconsin 1976.

33. Iooss, G. and Joseph, D. D., Elementary Stability and Bifurcation Theory, University of Minnesota Lecture Notes, 1979.

34. Sincovec, R. F. and Madsen, N. K., ACM-TOMS 1975 1 232.

NOTATION

a	cross-sectional area of the reactor, m^2
A	frequency factor, s^{-1}
B	dimensionless heat of reaction, $\Delta H c_0 / \rho C_p T_0$
c	concentration, mol/m^3
C_0	inlet concentration, mol/m^3
C_p	specific heat, J/mol°K
D	Damköhler number, $A e^{-\gamma} L/v$
D_e	effective diffusivity, m^2/s
E	activation energy, J/mol
ΔH	heat of reaction, J/mol
k_e	effective thermal conductivity J/s m°K
L	reactor length, m
P	reactor perimeter, m
Pe_m	Peclet number for mass transfer vL/D_e
Pe_h	Peclet number for heat transfer $\rho C_p vL/k_e$
R	universal gas constant
t	time, s
T	temperature, °K
T_0	inlet temperature, °K
s	dimensionless axial distance, x/L
U	heat transfer coefficient, $J/m^2 \cdot s°K$
v	velocity, m/s
x	axial distance, m
y	dimensionless concentration, c/c_0

Greek symbols

β dimensionless heat transfer coefficient, $UPL/av\rho C_p$

γ dimensionless activation energy, E/RT_0

θ dimensionless temperature, T/T_0

ρ density kg/m^3

τ dimensionless time, tv/L

SECURITY CLASSIFICATION OF THIS PAGE (When Data Entered)

REPORT DOCUMENTATION PAGE

READ INSTRUCTIONS BEFORE COMPLETING FORM

1. REPORT NUMBER: 2136	2. GOVT ACCESSION NO.: AD-A096653
3. RECIPIENT'S CATALOG NUMBER:	
4. TITLE (and Subtitle): NUMERICAL HOPF BIFURCATION TECHNIQUES AND THE DYNAMICS OF THE TUBULAR REACTOR MODEL	5. TYPE OF REPORT & PERIOD COVERED: Summary Report - no specific reporting period
	6. PERFORMING ORG. REPORT NUMBER:
7. AUTHOR(s): Robert F. Heinemann and Aubrey B. Poore	8. CONTRACT OR GRANT NUMBER(s): DAAG29-80-C-0041
9. PERFORMING ORGANIZATION NAME AND ADDRESS: Mathematics Research Center, University of Wisconsin, 610 Walnut Street, Madison, Wisconsin 53706	10. PROGRAM ELEMENT, PROJECT, TASK AREA & WORK UNIT NUMBERS: 2 Physical Mathematics
11. CONTROLLING OFFICE NAME AND ADDRESS: U. S. Army Research Office, P.O. Box 12211, Research Triangle Park, North Carolina 27709	12. REPORT DATE: November 1980
	13. NUMBER OF PAGES: 29
14. MONITORING AGENCY NAME & ADDRESS (if different from Controlling Office): Technical summary Rept.	15. SECURITY CLASS. (of this report): UNCLASSIFIED
	15a. DECLASSIFICATION/DOWNGRADING SCHEDULE:

16. DISTRIBUTION STATEMENT (of this Report)

Approved for public release; distribution unlimited.

17. DISTRIBUTION STATEMENT (of the abstract entered in Block 20, if different from Report)

18. SUPPLEMENTARY NOTES

19. KEY WORDS (Continue on reverse side if necessary and identify by block number)

Hopf bifurcation, chemical reactors, multiplicity, oscillations, stability

20. ABSTRACT (Continue on reverse side if necessary and identify by block number)

Numerical bifurcation techniques were developed for studying the multiplicity, stability, and oscillatory dynamics of the non-adiabatic tubular reactor with a single A→B reaction. The techniques illustrate the existence of one, three, five, or seven steady states and bifurcating periodic solutions. We present numerical procedures for computing the Hopf bifurcation formulas which can determine the stability and location of the oscillation without integrating the parabolic partial differential equations. The combination of our Hopf techniques with steady state bifurcation methods enables us to determine all possible steady and stable oscillatory solutions exhibited by distributed parameter models such as the tubular reactor.

DD FORM 1 JAN 73 1473 EDITION OF 1 NOV 65 IS OBSOLETE

S/N 0102-014-6601

UNCLASSIFIED

SECURITY CLASSIFICATION OF THIS PAGE (When Data Entered)

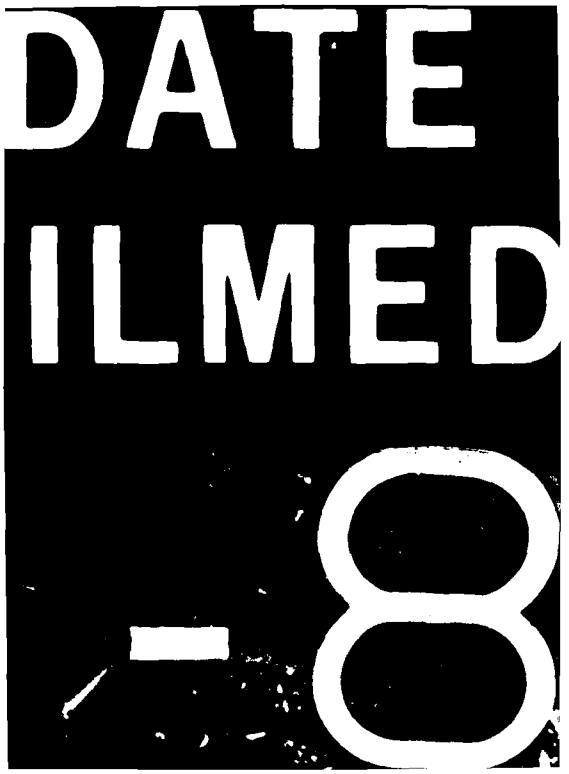
DATE
ILMED
-8